Hindawi
Journal of Applied Mathematics
Volume 2017, Article ID 1697135, 13 pages
https://doi.org/10.1155/2017/1697135

Research Article

Viscous Dissipation Effects on the Motion of Casson Fluid over an Upper Horizontal Thermally Stratified Melting Surface of a Paraboloid of Revolution: Boundary Layer Analysis

T. M. Ajayi, A. J. Omowaye, and I. L. Animasaun

Department of Mathematical Sciences, Federal University of Technology, Akure, Ondo State, Nigeria

Correspondence should be addressed to T. M. Ajayi; stillmetunde@gmail.com

Received 30 June 2016; Revised 20 October 2016; Accepted 6 November 2016; Published 4 January 2017

Academic Editor: Igor Andrianov

The problem of a non-Newtonian fluid flow past an upper surface of an object that is neither a perfect horizontal/vertical nor inclined/cone in which dissipation of energy is associated with temperature-dependent plastic dynamic viscosity is considered. An attempt has been made to focus on the case of two-dimensional Casson fluid flow over a horizontal melting surface embedded in a thermally stratified medium. Since the viscosity of the non-Newtonian fluid tends to take energy from the motion (kinetic energy) and transform it into internal energy, the viscous dissipation term is accommodated in the energy equation. Due to the existence of internal space-dependent heat source; plastic dynamic viscosity and thermal conductivity of the non-Newtonian fluid are assumed to vary linearly with temperature. Based on the boundary layer assumptions, suitable similarity variables are applied to nondimensionalized, parameterized and reduce the governing partial differential equations into a coupled ordinary differential equations. These equations along with the boundary conditions are solved numerically using the shooting method together with the Runge-Kutta technique. The effects of pertinent parameters are established. A significant increases in $\mathrm{Re}_x^{1/2} C_{fx}$ is guaranteed with S_t when magnitude of β is large. $\mathrm{Re}_x^{1/2} C_{fx}$ decreases with E_c and m.

1. Introduction

Within the last thirty years, the study of non-Newtonian fluid flow over a stretching surface has received significant attention due to its industrial applications. Such interest is fueled by its pertinent engineering applications in a number of fields as in spinning of filaments, continuous casting of metal, extrusion of polymers, crystal growing, glass fiber production, extrusion of plastic sheets, paper production, and process of condensation of metallic plates. Boundary layer analysis of fluid flow passing through a thick needle with variable diameter was investigated by Lee [1]. Historically, this can be referred to as the first report of flow adjacent to a surface with variable thickness where the effect of viscosity is highly significant. Thereafter, extensive studies were conducted on the boundary layer flows over a thin needle. Cebeci and Na [2] investigated the laminar free convection heat transfer from a needle. Ahmad et al. [3] examined the boundary layer flow over a moving thin needle with variable heat flux. The boundary layer flow over a stretching surface with variable thickness was analyzed by Fang et al. [4]. Recently, the flow of different fluids over an upper horizontal surface with variable thickness has been investigated extensively in [5–7]. This attracted Makinde and Animasaun [8, 9] to focus on the case of quartic autocatalysis kind of chemical reaction in the flow of an electrically conducting nanofluid containing gyrotactic-microorganism over an upper horizontal surface of a paraboloid of revolution in the presence and absence of thermophoresis and Brownian motion. In most cases, plastic dynamic viscosity of non-Newtonian Casson fluid tends to take energy away from the motion and transform it into internal energy. However, this area has been neglected.

In fluid mechanics, destruction of fluctuating velocity gradients due to viscous stresses is known as viscous dissipation. This partial irreversible processes is often referred to as transformation of kinetic energy into internal energy of the fluid (heating up the fluid due to viscosity since dissipation is high in the regions with large gradients). Pop [10] remarked that understanding the concept of energy dissipation and transport in nanoscale structures is of great importance for the design of energy-efficient circuits and energy-conversion systems. However, energy dissipation and transport of non-Newtonian fluid are also of importance to engineers and scientists. Motsumi and Makinde [11] examined the effects of viscous dissipation parameter (i.e., Eckert number), thermal diffusion, and thermal radiation on boundary layer flow of Cu-water and Al_2O_3-water nanofluids over a moving flat plate. In another theoretical study on combined effects of Newtonian heating and viscous dissipation parameter on boundary layer flow of copper and titania in water over stretchable wall, Makinde [12] reported an increase in the moving plate surface temperature and thermal boundary layer thickness. Depending on the admissible grouping of variables (parameterization), Eckert number and Brinkmann number ($Pr \times E_c$) may be used to quantify viscous dissipation. In addition, unsteady mixed convection in the flow of air over a semi-infinite stretching sheet taking into account the effect of viscous dissipation was carried out by Abd El-Aziz [13]. Both at steady stage ($A = 0$) and unsteady stage ($A = 1.5$), velocity and temperature of the flow increase with an increase in the magnitude of Eckert number. Recently, effects of viscous dissipation, Joule heating, and partial velocity slip on two-dimensional stagnation point flow were reported by Yasin et al. [14]. In another study conducted by Animasaun and Aluko [15], it is reported that when dynamic viscosity of air is assumed to vary linearly with temperature, normal negligible effect of Eckert number on velocity profiles will be noticed. Raju and Sandeep [16] focused on the motion of Casson fluid over a moving wedge with slip and observed a decrement in the temperature field with rising values of Eckert number. In the flow of non-Newtonian Casson fluid over an upper horizontal thermally stratified melting surface of a paraboloid of revolution, dissipation of smaller eddies due to molecular viscosity near the wall is significant. In the presence of constant magnetic field, electrically conducting Casson fluid flow over object that is neither a perfect horizontal/vertical nor inclined/cone is also an important issue.

The study of electrically conducting fluid flow is of considerable interest in modern metallurgical. This can be traced to the fact that most fluids in this sector are electrically conducting fluid. Historically, the first report on the motion of electrically conducting fluid in the presence of magnetic field was presented by Rossow [17]. Thereafter, Alfvén [18] reported that if a conducting liquid is placed in a constant magnetic field, every motion of the liquid generates a force called electromotive force (e.m.f.) which produces electric currents. One of the most significant importance of these contributions are its applications in engineering problems such as MHD generators, plasma studies, nuclear reactors, and geothermal energy extractions. Soundalgekar and Murty [19] investigated heat transfer in MHD flow with pressure gradient, suction, and injection. It was observed that an increase in the magnetic field parameter leads to an increase in fluid velocity, skin friction, rate of heat transfer, and a fall in temperature. Rajeswari et al. [20] observed that, due to the uniform magnetic field and suction at the wall of the surface, the concentration of the fluid decreases with the increase in chemical reaction parameter. Ghosh et al. [21] found that an increase in inclination of the applied magnetic field opposes primary flow and also reduces Grashof numbers. Das [22] concluded that increasing magnetic field and thermal radiation leads to deceleration of velocity but reverse is the effect for the melting parameter when the solid surface and the free stream move in the same direction. Motsa and Animasaun [23] presented the behavior of unsteady non-Darcian magnetohydrodynamic fluid flow past an impulsively using bivariate spectral local linearization analysis. Koriko et al. [24] illustrated the dynamics of two-dimensional magnetohydrodynamics (MHD) free convective flow of micropolar fluid along a vertical porous surface embedded in a thermally stratified medium. It was concluded that velocity profiles and microrotation profiles are strongly influenced by the magnetic field in the boundary layer, which decreases with an increase in the magnitude of magnetic parameter. Recently, theoretical investigation of MHD natural convection flow in vertical microchannel formed by two electrically nonconducting infinite vertical parallel plates and effects of MHD mixed convection on the flow through vertical pipe with time periodic boundary condition was presented explicitly by Jha and Aina [25, 26].

Several processes involving melting heating transfer in non-Newtonian fluids have promising applications in thermal engineering, such as melting permafrost, oil extraction, magma solidification, and thermal insulation. As such, a lot of experimental and theoretical work has been conducted in the kinetics of heat transfer accompanied with melting or solidification effect. The process of melting of ice placed in a hot stream of air at a steady state was first reported by Roberts [27]. Historically, this report can be referred to as the pioneering analysis of the melting phenomenon. Another novel report on melting phenomenon during forced convection heat transfer when an iceberg drifts in warm sea water was presented by Tien and Yen [28]. From their investigation, they observed that melting at the interface results in a decrease in the Nusselt number. Epstein and Cho [29] discussed the laminar film condensation on a vertical surface. Much later, melting heat transfer in a nanofluid boundary layer on a stretching circular cylinder was examined by Gorla et al. [30]. In the study of the effect of radiation on MHD mixed convection flow from a vertical plate embedded in a saturated porous media with melting, Adegbie et al. [31] reported that the Nusselt number decreases with increase in melting parameter. Adegbie et al. [31] stated that the temperature of UCM fluid flow over a melting surface is an increasing function of variable thermal conductivity parameter. Omowaye and Animasaun [32] investigated boundary layer analysis in the flow of upper convected Maxwell fluid flow. Due to the fact that temperature at the wall is zero, classical temperature-dependent viscosity and thermal conductivity linear models were modified to suit the case of both melting heat transfer

and thermal stratification. In another study of micropolar fluid flow in the presence of temperature-dependent and space heat source, the analysis of the case where vortex viscosity is a constant function of temperature was reported in [33].

Within the past two decades, the effects of temperature-dependent viscosity on the fluid flow have become more important to engineers dealings with geothermal systems, crude oil extraction, and machinery lubrication. Due to friction and internal heat generated between two layers of fluid, viscosity and thermal conductivity of fluid substance may be affected by temperature; for more details see Batchelor [34], Lai and Kulacki [35], and Abd El-Aziz [36]. Proper consideration of this fact in the study on inherent irreversibility in a variable viscosity Couette flow by Makinde and Maserumule [37], numerical investigation of micropolar fluid flow over a nonlinear stretching sheet taking into account the effects of a temperature-dependent viscosity by Rahman et al. [38], effects of MHD on Casson fluid flow in the presence of Cattaneo-Christov heat flux by Malik et al. [39], fluid flow through a pipe with variation in viscosity by Makinde [40], Casson fluid flow within boundary layer over an exponentially stretching surface embedded in a thermally stratified medium by Animasaun [41], steady fully developed natural convection flow in a vertical annular microchannel having temperature-dependent viscosity in the presence of velocity slip and temperature jump at the annular microchannel surfaces by Jha et al. [42] have enhanced the body of knowledge on fluid flow, boundary layer analysis, and heat/mass transfer. In a recent experiment, Alam et al. [43] concluded that thermal boundary layer decreases with an increasing temperature-dependent viscosity. Hayat et al. [44] discussed the effect of variable thermal conductivity on the mixed convective flow over a porous medium stretching surface. In the article, the kinematics viscosity of Casson fluid was considered as a function depending on plastic dynamic viscosity, density, and Casson parameter and hence reported that increase in the magnitude of temperature-dependent viscosity parameter leads to an increase in fluid's velocity. The above literature review shows that there exists no published article on the effects of viscous dissipation in the flow of non-Newtonian Casson fluid over a upper horizontal thermally stratified melting surface of a paraboloid of revolution.

2. Formulation of the Problem

Consider a steady, incompressible, laminar flow of an electrically conducting non-Newtonian (Casson) fluid over a melting surface on upper horizontal paraboloid of revolution in the presence of viscous dissipation and thermal stratification. The x-axis is taken in the direction of motion and y-axis is normal to the flow as shown in Figures 1(a) and 1(b). A uniform magnetic field of strength B_o is applied normal to the flow. The induced magnetic field due to the motion of an electrically conducting Casson fluid is assumed to be so small; hence it is neglected. The stretching velocity is $U_w = U_o(x+b)^m$ and the wall is assumed impermeable. It is further assumed that the immediate fluid layer adjacent to the surface is specified as $y = A(x+b)^{(1-m)/2}$, where $m < 1$. Using Boussinesq approximation, the difference in inertia is negligible but gravity is sufficiently strong to make the specific weight appreciably different between any two layers of Casson fluid on the surface; hence the rate flow on this kind of surface is referred to as free convection. The body force term suitable to induce the flow over a surface which is neither a perfect horizontal/vertical nor inclined/cone is

$$-\frac{\partial p}{\partial x} + \rho g_x = g\gamma \frac{m+1}{2}\left(T_\infty - T\right) + 0. \tag{1}$$

Following the theory stated in Casson [45] and boundary layer assumptions, the rheological equation for an isotropic Casson fluid flow together with heat transfer is of the form

$$\frac{\partial u}{\partial x} + \frac{\partial v}{\partial y} = 0, \tag{2}$$

$$u\frac{\partial u}{\partial x} + v\frac{\partial u}{\partial y} = \frac{1}{\rho}\left(1+\frac{1}{\beta}\right)\frac{\partial}{\partial y}\left(\mu_b(T)\frac{\partial u}{\partial y}\right) + g\gamma \cdot \frac{m+1}{2}\left(T_\infty - T\right) - \frac{\sigma B_o^2}{\rho}u, \tag{3}$$

$$u\frac{\partial T}{\partial x} + v\frac{\partial T}{\partial y} = \frac{1}{\rho Cp}\frac{\partial}{\partial y}\left(\kappa_b(T)\frac{\partial T}{\partial y}\right) + \frac{\mu_b(T)}{\rho Cp}\left(1+\frac{1}{\beta}\right)\frac{\partial u}{\partial y}\frac{\partial u}{\partial y} + \frac{Q_o\left[T_w(x) - T_\infty\right]}{\rho C_p} \cdot \exp\left[-ny\sqrt{\frac{m+1}{2}}\sqrt{\frac{U_o}{\vartheta}}(x+b)^{(m-1)/2}\right]. \tag{4}$$

Suitable boundary conditions governing the flow along upper horizontal surface of a paraboloid of revolution are

$$\begin{aligned} u &= U_o(x+b)^m, \\ \kappa_b(T)\frac{\partial T}{\partial y} &= \rho\left[\lambda^* + c_s\left(T_m - T_o^*\right)\right]v(x,y), \\ T &= T_m(x) \qquad \text{at } y = A(x+b)^{(1-m)/2}, \end{aligned} \tag{5}$$

$$\begin{aligned} u &\longrightarrow 0, \\ T &\longrightarrow T_\infty(x) \qquad \text{as } y \longrightarrow \infty. \end{aligned} \tag{6}$$

The formulation of the second term in boundary (5) states that the heat conducted to the melting surface on paraboloid of revolution is equal to the combination of heat of melting and the sensible heat required to raise the solid temperature T_o to its stratified melting temperature $T_m(x)$ (for details, see [29]). For lubricating fluids, heat generated by the internal friction and the corresponding increase in temperature affects the viscosity of the fluid; hence, it may not be realistic to constant function of plastic dynamic viscosity knowing fully well that space-dependent internal heat source is significant. In order to account for this variation, it is valid to consider the modified mathematical models of both the

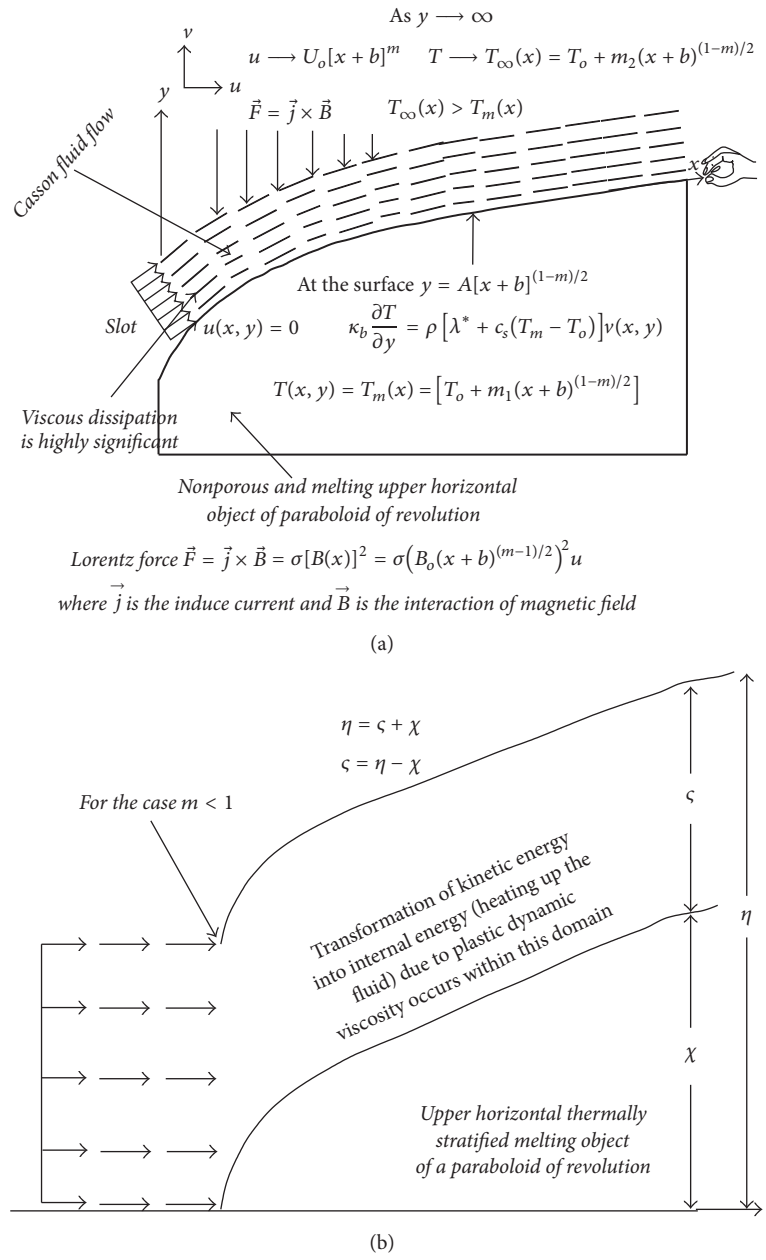

FIGURE 1: (a) The coordinate system of Casson fluid flow over upper horizontal thermally stratified melting surface of a paraboloid of revolution. (b) Graphical illustration of fluid domain and conversion of domain from $[\chi, \infty)$ to $[0, \infty)$.

temperature-dependent viscosity and thermal conductivity models proposed in [46] and adopted in [31, 32] as

$$\begin{aligned} \mu_b(T) &= \mu_b^*\left[1 + b_1(T_\infty - T)\right], \\ \kappa_b(T) &= \kappa_b^*\left[1 + b_2(T - T_m)\right], \\ \theta(\eta) &= \frac{T - T_m}{T_\infty - T_o}. \end{aligned} \tag{7}$$

Meanwhile, the models are still in good agreement with experimental data of Batchelor [34]. It is worth mentioning that the first and second terms in (7) are valid and reliable since $T_\infty(x) > T_m(x)$ in this study, whereas thermal stratification (T_m) at the melting wall and at the free stream is defined as

$$\begin{aligned} T_m(x) &= T_o + m_1(x+b)^{(1-m)/2}, \\ T_\infty(x) &= T_o + m_2(x+b)^{(1-m)/2}. \end{aligned} \tag{8}$$

Using similarity variable for temperature $\theta(\eta)$ in (7) to simplify $[1 - \theta(\eta)]$ we obtain suitable temperature difference in flow past thermally stratified horizontal melting surface of paraboloid of revolution as

$$T_\infty - T = (1 - \theta)\left[T_\infty - T_o\right] - m_1(x+b)^{(1-m)/2}. \tag{9}$$

From thermal stratification models in (9), the following relations can be easily obtained

$$b_1 (T_m - T_o) = b_1 m_1 (x+b)^{(1-m)/2}, \quad b_1 (T_\infty - T_o) = b_1 m_2 (x+b)^{(1-m)/2}, \tag{10}$$

where T_o is known as reference temperature. A significant difference between $(T_m - T_o)$ and $(T_\infty - T_o)$ can be easily obtained from (10). This can be traced to the fact that the linear stratification occurs at all points of "x" on the wall $(y = A(x+b)^{(1-m)/2})$ and at all points of "x" at the free stream as $(y \to \infty)$. In view of this, it is valid to define temperature-dependent viscous parameter ξ by considering the second term in (10) since $T_\infty(x) > T_m(x)$. Mathematically, the ratio of the first two terms in (10) can thus produce dimensionless thermal stratification parameter (S_t) as

$$\xi = b_1 (T_\infty - T_o), \quad b_1 (T_m - T_o) = \xi S_t, \quad S_t = \frac{m_1}{m_2}. \tag{11}$$

The stream function $\psi(x, y)$ and similarity variable η are of the form

$$u = \frac{\partial \psi}{\partial y}, \quad v = -\frac{\partial \psi}{\partial x}, \quad \eta = y\left(\frac{m+1}{2}\frac{U_o}{\vartheta}\right)^{1/2}(x+b)^{(m-1)/2}, \quad \psi = f\left(\frac{2}{m+1}\right)^{1/2}(\vartheta U_o)^{1/2}(x+b)^{(m+1)/2}. \tag{12}$$

It is important to note that the stream function $\psi(x, y)$ automatically satisfies continuity (2). The nonlinear partial differential equations (3) and (4) are reduced to the following nonlinear coupled ordinary differential equations

$$\begin{aligned}
&[1+\xi-\theta\xi-\xi S_t]\left(1+\frac{1}{\beta}\right)\frac{d^3 f}{d\eta^3} - \xi\left(1+\frac{1}{\beta}\right)\frac{d\theta}{d\eta}\frac{d^2 f}{d\eta^2} + f\frac{d^2 f}{d\eta^2} - \frac{2m}{m+1}\frac{df}{d\eta}\frac{df}{d\eta} \\
&+ \frac{2H_a}{m+1}\frac{df}{d\eta} + G_t[(1-\theta)\xi - \xi S_t] = 0, \\
&[1+\varepsilon\theta]\frac{d^2\theta}{d\eta^2} + \varepsilon\frac{d\theta}{d\eta}\frac{d\theta}{d\eta} - P_r S_t\frac{1-m}{m+1}\frac{df}{d\eta} + P_r f\frac{d\theta}{d\eta} \\
&- P_r\frac{1-m}{m+1}\theta\frac{df}{d\eta} + P_r E_c\frac{m+1}{2}[1+\xi-\theta\xi-\xi S_t]\left(1+\frac{1}{\beta}\right)\frac{d^2 f}{d\eta^2}\frac{d^2 f}{d\eta^2} \\
&+ \frac{2P_r\Gamma}{m+1}e^{[-n\eta]} = 0.
\end{aligned} \tag{13, 14}$$

In (13) and (14), melting parameter δ, Prandtl number P_r, magnetic parameter H_a, Eckert number E_c, temperature-dependent thermal conductivity parameter ε, space-dependent internal heat source parameter Γ, skin friction coefficient C_{fx}, Nusselt number Nu_x, and buoyancy parameter depending on volumetric-expansion coefficient due to temperature G_t are defined as

$$\begin{aligned}
E_c &= \frac{U_o^2 (x+b)^{(m+1)/2}}{C_p (T_w - T_\infty)}, \\
\delta &= \frac{C_p m_2 (x+b)^{(1-m)/2}}{\left[\lambda^* + c_s m_1 (x+b)^{(1-m)/2}\right]}, \\
H_a &= \frac{\sigma B_o^2}{\rho U_o}, \\
\varepsilon &= b_2 (T_\infty - T_o), \\
\Gamma &= \frac{Q_o}{\rho C_p U_o (x+b)^{m-1}}, \\
G_t &= \frac{g\gamma}{b_1 U_o^2 (x+b)^{2m-1}}, \\
C_{fx} &= \frac{\tau_w}{\rho\sqrt{(m+1)/2}\,(U_w)^2}, \\
\mathrm{Nu}_x &= \frac{(x+b)\,q_w}{\kappa_b [T_\infty - T_o]\sqrt{(m+1)/2}},
\end{aligned} \tag{15}$$

where τ_w is the shear stress (skin friction) between Casson fluid and upper surface of horizontal paraboloid of revolution and q_w is the heat flux at all points on the surface

$$\tau_w = \mu_b\left(1+\frac{1}{\beta}\right)\left.\frac{\partial u}{\partial y}\right|_{y=A(x+b)^{(1-m)/2}}, \quad q_w = -\left(\kappa_b\left.\frac{\partial T}{\partial y}\right|_{y=A(x+b)^{(1-m)/2}}\right). \tag{16}$$

In order to nondimensionalize the boundary conditions (5) and (6), it is pertinent to note that the minimum value of y is not the starting point of the slot. This implies that all the conditions in (5) are not imposed at $y = 0$. As shown in Figures 1(a) and 1(b), it is obvious that it may not be realistic to say that $y = 0$ at all points on upper horizontal melting surface of a paraboloid of revolution. Hence, it is not valid to set $y = 0$ in similarity variable η. Upon using $y = A(x+b)^{(1-m)/2}$ the minimum value of y which accurately corresponds to minimum value of similarity variable

$$\eta = A\left(\frac{m+1}{2}\frac{U_o}{\vartheta}\right)^{1/2} = \chi. \tag{17}$$

This implies that, at the surface ($y = A(x+b)^{(1-m)/2}$), the boundary condition suitable to scale the boundary layer flow is $\eta = \chi$. The boundary condition becomes

$$\begin{aligned} \frac{df}{d\chi} &= 0, \\ f(\chi) + \frac{\delta[1+\theta\varepsilon]}{P_r}\frac{d\theta}{d\chi} + \chi\frac{m-1}{m+1}\frac{df}{d\chi} &= 0, \\ \theta(\chi) &= 0 \\ &\text{at } \chi = \eta. \end{aligned} \tag{18}$$

$$\begin{aligned} \frac{df}{d\chi} &\longrightarrow 1, \\ \theta(\chi) &\longrightarrow 1 - S_t \\ &\text{as } \chi \longrightarrow \infty. \end{aligned} \tag{19}$$

Moreover, dimensionless governing equations (13) and (14) are depending on η while the boundary conditions (18) and (19) are functions and/or derivatives depending on χ. In order to transform the domain from $[\chi, \infty)$ to $[0, \infty)$ it is valid to adopt $F(\varsigma) = F(\eta - \chi) = f(\eta)$ and $\Theta(\varsigma) = \Theta(\eta - \chi) = \theta(\eta)$; for more details, see Figure 1(b). Considering the fact that Prandtl number is strongly dependent on plastic dynamic viscosity and thermal conductivity, and it is assumed that both properties vary linearly with temperature; hence for more accurate analysis of boundary layer as suggested in [47, 48], the P_r in (14) is

$$\begin{aligned} P_r &= \frac{\mu_b C_p}{\kappa_b^*} = \left[1 + \xi - \theta\xi - \xi S_t\right]\frac{\mu_b^* C_p}{\kappa_b^*} \\ &= P_{r\infty}\left[1 + \xi - \theta\xi - \xi S_t\right] \end{aligned} \tag{20}$$

Equation (18) reveals that Prandlt number at free stream is denoted as $P_{r\infty}$. The final dimensionless governing equation (coupled system of nonlinear ordinary differential equation) is

$$\begin{aligned} &\left[1 + \xi - \Theta\xi - \xi S_t\right]\left(1 + \frac{1}{\beta}\right)\frac{d^3F}{d\varsigma^3} - \xi\left(1 + \frac{1}{\beta}\right)\frac{d\Theta}{d\varsigma}\frac{d^2F}{d\varsigma^2} + F\frac{d^2F}{d\varsigma^2} - \frac{2m}{m+1}\frac{dF}{d\varsigma}\frac{dF}{d\varsigma} \\ &+ \frac{2H_a}{m+1}\frac{dF}{d\varsigma} + G_t\left[(1-\Theta)\xi - \xi S_t\right] = 0, \\ &\left[1 + \varepsilon\Theta\right]\frac{d^2\Theta}{d\varsigma^2} + \varepsilon\frac{d\Theta}{d\varsigma}\frac{d\Theta}{d\varsigma} + \left[1 + \xi - \Theta\xi - \xi S_t\right] \\ &\cdot\left(-P_{r\infty}S_t\frac{1-m}{m+1}\frac{dF}{d\varsigma} + P_{r\infty}F\frac{d\Theta}{d\varsigma} - P_{r\infty}\frac{1-m}{m+1}\Theta\frac{dF}{d\varsigma}\right) + P_{r\infty}E_c\frac{m+1}{2}\left[1 + \xi - \Theta\xi - \xi S_t\right]^2\left(1 + \frac{1}{\beta}\right)\frac{d^2F}{d\varsigma^2}\frac{d^2F}{d\varsigma^2} + P_{r\infty}\left[1 + \xi - \Theta\xi - \xi S_t\right]\frac{2\Gamma}{m+1}e^{[-n\varsigma]} = 0. \end{aligned} \tag{21}$$

Due to the fact that $\Theta(\varsigma) = 0$, the influence of temperature-dependent thermal conductivity on heat conduction during melting process diminishes. Dimensionless boundary condition reduces to

$$\begin{aligned} \frac{dF}{d\varsigma} &= 0, \\ F(\varsigma) + \frac{\delta}{P_{r\infty}\left[1 + \xi - \xi S_t\right]}\frac{d\Theta}{d\varsigma} + \chi\frac{m-1}{m+1}\frac{dF}{d\varsigma} &= 0, \\ \Theta(\varsigma) &= 0 \\ &\text{at } \varsigma = 0. \end{aligned} \tag{22}$$

$$\begin{aligned} \frac{dF}{d\varsigma} &\longrightarrow 1, \\ \Theta(\varsigma) &\longrightarrow 1 - S_t \\ &\text{as } \varsigma \longrightarrow \infty. \end{aligned} \tag{23}$$

Upon substituting the similarity variables (12) and models of physical quantities (i.e., C_{fx} and Nu_x) at the wall into (16) we obtain

$$\begin{aligned} \mathrm{Re}_x^{1/2}C_{fx} &= \left(1 + \frac{1}{\beta}\right)F''(0), \\ \mathrm{Nu}_x\mathrm{Re}_x^{-1/2} &= -\Theta'(0). \end{aligned} \tag{24}$$

3. Numerical Solution

Numerical solutions of the boundary valued problem (21)–(24) are obtained using classical Runge-Kutta method with shooting techniques and MATLAB package (`bvp5c`). The boundary value problem cannot be solved on an infinite interval and it would be impractical to solve it for even a very large finite interval; hence ς at infinity is 10. Using the method of superposition by Na [49], the boundary value problem of ODE has been reduced to a system of five simultaneous equations of first order (IVP) for five unknowns following the method of superposition. In order to integrate the corresponding IVP, the values of $F''(\varsigma = 0)$ and $\Theta'(\varsigma = 0)$ are required. However, such values do not exist after the nondimensionalization of the boundary conditions (5) and (6). The suitable guess values for $F''(\varsigma = 0)$ and $\Theta'(\varsigma = 0)$ are chosen and then integration is carried out. The calculated values of $F'(\varsigma)$ and $\Theta(\varsigma)$ at infinity ($\varsigma = 10$) are compared with the given boundary conditions in (24) and the estimated values $F''(\varsigma = 0)$ and $\Theta'(\varsigma = 0)$ are adjusted to give a better approximation for the solution. Series of values for $F''(\varsigma = 0)$ and $\Theta'(\varsigma = 0)$ are considered and applied with fourth-order classical Runge-Kutta method using step size $\Delta\varsigma = 0.01$.

Table 1: Validation of numerical technique: comparison between the solutions of classical Runge-Kutta together with shooting (RK4SM) and MATLAB solver bvp5c for the limiting case.

S_t	$F''(\varsigma = 0)$ (RK4SM)	$F''(\varsigma = 0)$ (bvp5c)	$\Theta'(\varsigma = 0)$ (RK4SM)	$\Theta'(\varsigma = 0)$ (bvp5c)
0	0.140452622100684	0.140452622451879	2.244340556008000	2.244340556781432
0.5	0.140381952095092	0.140381952471126	2.090185332523411	2.090185332413216
1	0.140582481552633	0.140582481451697	1.932324537463769	1.932324537412539

The above procedure is repeated until asymptotically converged results are obtained within a tolerance level of 10^{-6}. It is very important to remark that setting $\varsigma_\infty = 10$, all profiles are compatible with the boundary layer theory and asymptotically satisfies the conditions at free stream as suggested by Pantokratoras [50]. It is worth mentioning that there exist no related published articles that can be used to validate the accuracy of the numerical results. In view of this, (21)–(24) can easily be solved using ODE solvers such as MATLAB's bvp5c as explained in Kierzenka and Shampine [51] and Gökhan [52].

3.1. Verification of the Results. In order to verify the accuracy of the present analysis, the results of classical Runge-Kutta together with shooting have been compared with that of bvp5c solution for the limiting case when $\xi = 0.07$, $\varepsilon = 0.1$, $\beta = 0.1$, $E_c = 0.3$, $H_a = 0.25$, $\Gamma = 1$, $n = 0.09$, $P_{r\infty} = 1$, $m = 0.17$, $\delta = 0.2$, $\chi = 0.3$, and $G_t = 1$ at various values of S_t within the range $0 \le S_t \le 1$. As shown in Table 1, the comparison in the above case is found to be in good agreement. This good agreement is an encouragement for further study of the effects of other parameters.

4. Results and Discussion

The numerical computations have been carried out for various values of major parameters using the numerical scheme discussed in the previous section. This section presents the effect of different embedded physical parameters on the flow. Following Mustafa et al. [53], the ratio of momentum diffusivity to thermal diffusivity is considered to be unity (i.e., $P_r = 1$) due to the fact that Casson fluid flow under consideration possesses substantial yield stress.

4.1. Influence of Velocity Index Parameter m and Eckert Number E_c. At metalimnion level of thermal stratification ($S_t = 0.5$), when $\xi = 0.07$, $\varepsilon = 0.1$, $\beta = 0.1$, $E_c = 0.3$, $H_a = 0.25$, $\Gamma = 1$, $n = 0.09$, $P_{r\infty} = 1$, $\delta = 0.2$, $\chi = 0.3$, and $G_t = 1$, it is worth noting that both vertical and horizontal velocities decrease with m; see Figures 2 and 3. Combination of these practical meanings of velocity index parameter m justifies the decrease in both vertical and horizontal velocities profiles we obtained. Meanwhile, temperature distribution within the flow increases with m from a few distance after wall till free stream; see Figure 4. With an increase in the magnitude of m, Figure 5 reveals that temperature gradient profile $\Theta'(\varsigma)$ increases near the wall $0 \le \varsigma \le 3.1$ and decreases thereafter as $\varsigma \to 10$. It is very important to notice that velocity profile when $m = 0.15$ perfectly satisfies free stream condition asymptotically. This can be traced to the fact that

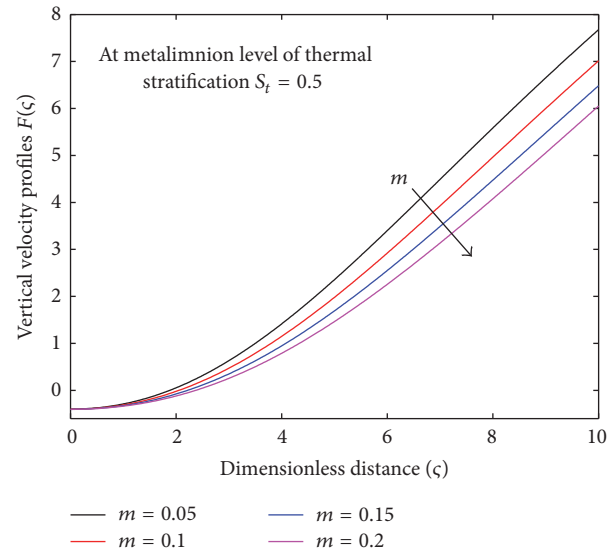

Figure 2: Effect of m on $F(\varsigma)$.

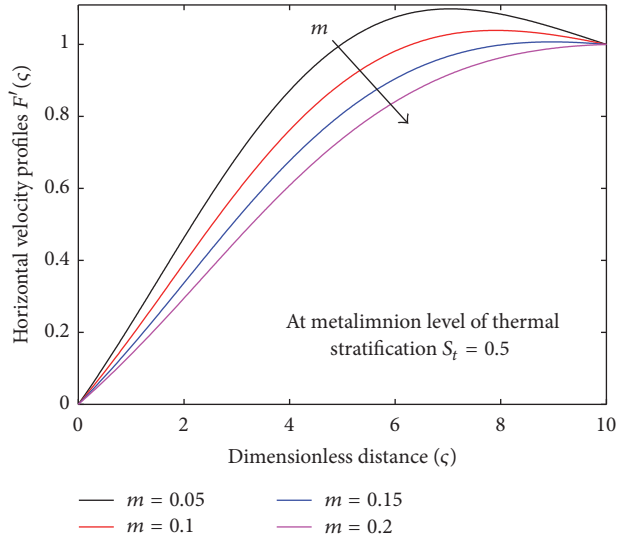

Figure 3: Effect of m on $F'(\varsigma)$.

$\Theta(0) = 0$ and as $\varsigma \to 10$, $\Theta(\varsigma) \to 1 - S_t$. In addition, graphical illustration of the function which describes the immediate layer of Casson fluid next to an upper horizontal surface of a paraboloid of revolution $y = A(x + b)^{(1-m)/2}$ against x (i.e., $A = 1$ and $b = 0.8$) at various values of m less than 1 and stretching velocity at the wall $U_w = U_o(x + b)^m$ when stretching rate (i.e., $U_o = 3$) are presented in

Table 2: Variations in Nusselt number $\mathrm{Nu}_x\mathrm{Re}_x^{-1/2}$ with Eckert number at various values of velocity index parameter when $\xi = 0.07$, $\varepsilon = 0.1$, $\beta = 0.1$, $E_c = 0.3$, $H_a = 0.25$, $\Gamma = 1$, $n = 0.09$, $P_{r\infty} = 1$, $S_t = 0.5$, $\delta = 0.2$, $\chi = 0.3$, and $G_t = 1$.

E_c	$\mathrm{Nu}_x\mathrm{Re}_x^{-1/2}$ When $m = 0.05$	$\mathrm{Nu}_x\mathrm{Re}_x^{-1/2}$ When $m = 0.15$	$\mathrm{Nu}_x\mathrm{Re}_x^{-1/2}$ When $m = 0.25$	$\mathrm{Nu}_x\mathrm{Re}_x^{-1/2}$ When $m = 0.35$
0	−1.9834	−2.0331	−2.0471	−2.0414
1	−2.2543	−2.2092	−2.1769	−2.1460
2	−2.4838	−2.3594	−2.2869	−2.2333
3	−2.6799	−2.4879	−2.3799	−2.3055
4	−2.8485	−2.5981	−2.4582	−2.3646
5	−2.9940	−2.6924	−2.5237	−2.4120

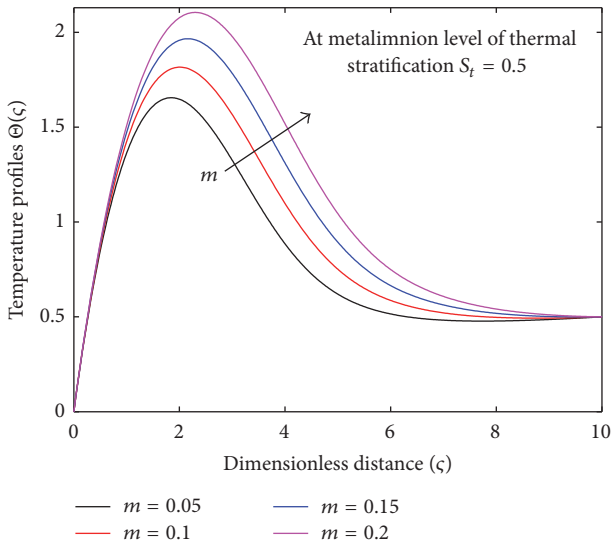

Figure 4: Effect of m on $\Theta(\varsigma)$.

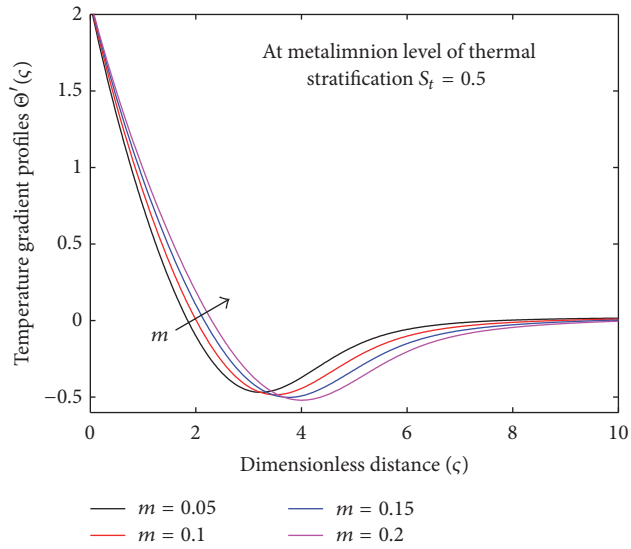

Figure 5: Effect of m on $\Theta'(\varsigma)$.

Figure 6. It is noticed that as m increases within $0.05 \leq m \leq 0.2$, the thickness of the paraboloid of revolution decreases but corresponding influence of stretching on the flow is an increasing function. The variation in local skin friction coefficient and local Nusselt number which is proportional to local heat transfer rate as stated in (25) as a function of viscous dissipation term and velocity index parameter is shown in Figure 7 and Table 2. Figure 7 shows that, at a fixed value of m, $\mathrm{Re}_x^{1/2}C_{fx}$ decreases with Eckert number E_c. At constant value of E_c, unequal decrease in $\mathrm{Re}_x^{1/2}C_{fx}$ with m is also observed. In addition, $\mathrm{Nu}_x\mathrm{Re}_x^{-1/2}$ decreases with E_c at various values of m. Table 2 shows that $\mathrm{Nu}_x\mathrm{Re}_x^{-1/2}$ increases highly significant when magnitude of E_c is large.

4.2. Influence of Non-Newtonian Casson Parameter β, Thermal Stratification Parameter S_t, and Eckert Number E_c. Figures 8–12 illustrate the effect of increasing the magnitude of non-Newtonian Casson parameter β on all the five profiles when $\xi = 0.07$, $\varepsilon = 0.1$, $E_c = 2$, $H_a = 0.25$, $\Gamma = 1$, $n = 0.09$, $P_{r\infty} = 1$, $m = 0.35$, $S_t = 0.5$, $\delta = 0.2$, $\chi = 0.3$, and $G_t = 1$. With an increase in the magnitude of β, it is observed that vertical velocity decreases, horizontal velocity decreases, temperature distribution increases only within the fluid domain ($2 \leq \varsigma \leq 8$), and the temperature gradient increases only near the wall. Figure 10 reveals that a distinct significant increase in $\mathrm{Re}_x^{1/2}C_{fx}$ is guarantee with an initial increase in β from 0.2 to 0.25. Physically, increase in the magnitude of non-Newtonian Casson parameter ($\beta \to \infty$ implies sharp transition in the flow behavior from non-Newtonian fluid flow to Newtonian fluid flow. In view of this, resistance in the fluid flow is produced. It is worth mentioning that an increase in β implies a decrease in yield stress P_y of the Casson fluid and increase in the magnitude of plastic dynamic viscosity μ_b.

It is observed that the present study complements related studies on Casson fluid flow with temperature-dependent plastic dynamic viscosity on nonmelting surface; see Figures 8 and 9 in [41], Figures 3 and 4 in [54], and Figure 2 reported by Jasmine Benazir et al. [55]. The relationship between non-Newtonian Casson parameter β and Eckert number is sought for and illustrated graphically in Figures 13 and 14. Within $0 \leq E_c \leq 1.5$, there exists no significant difference in $\mathrm{Re}_x^{1/2}C_{fx}$ with β. As shown in Figure 13, when the magnitude of $\beta = 0.25$, a distinct significant increase in $\mathrm{Re}_x^{1/2}C_{fx}$ is observed due to an increase in the magnitude of viscous dissipation parameter. At small magnitude of β, local Nusselt number ($\mathrm{Nu}_x\mathrm{Re}_x^{-1/2}$) which is proportional to local heat transfer rate is found to be decreasing with E_c. At large value of β,

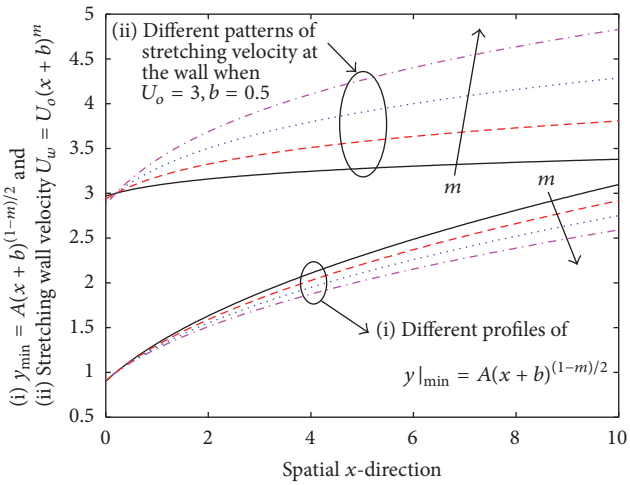

FIGURE 6: Graphical illustrations of (i) $y_{\min} = A(x+b)^{(1-m)/2}$; (ii) stretching wall velocity $U_w = U_o(x+b)^m$ at various values of m.

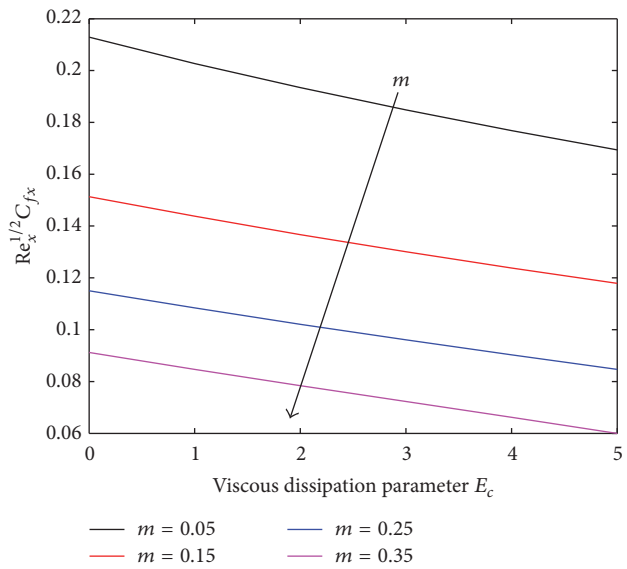

FIGURE 7: Variations in $\mathrm{Re}_x^{1/2}C_{fx}$ with E_c at various values of m.

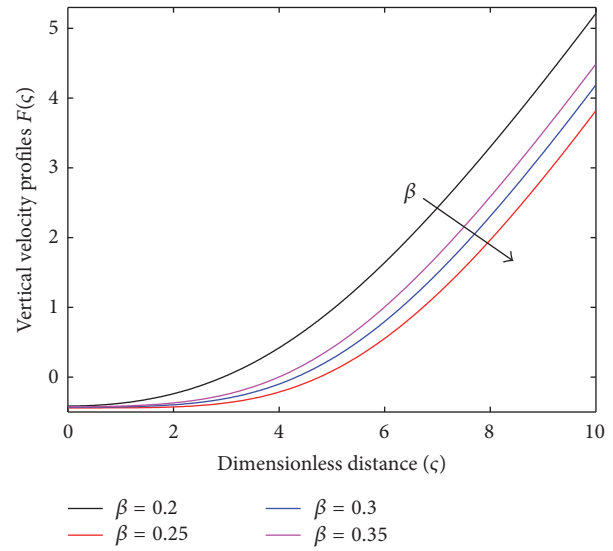

FIGURE 8: Effect of β on $F(\varsigma)$.

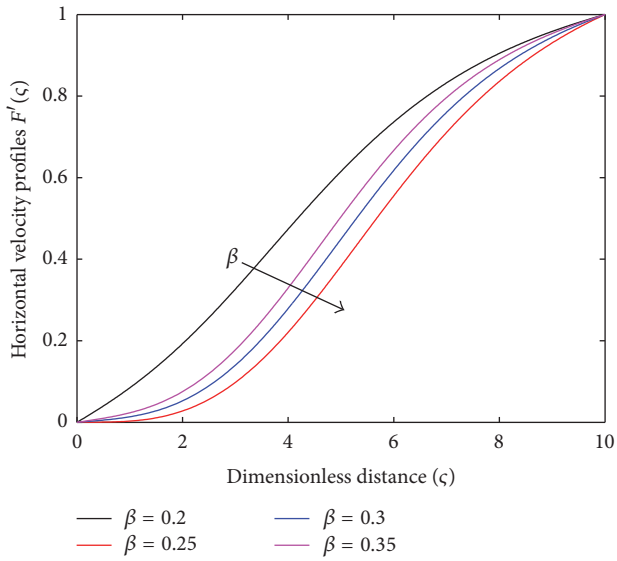

FIGURE 9: Effect of β on $F'(\varsigma)$.

$\mathrm{Nu}_x\mathrm{Re}_x^{-1/2}$ increases with E_c; see Figure 14. The simulation was further extended to unravels the relationship between non-Newtonian Casson parameter β, thermal stratification parameter S_t, and local skin friction coefficients when $\xi = 0.07$, $\varepsilon = 0.1$, $E_c = 2$, $H_a = 0.25$, $\Gamma = 1$, $n = 0.09$, $P_{r\infty} = 1$, $m = 0.17$, $\delta = 0.2$, $\chi = 0.3$, and $G_t = 1$. It is revealed in Figure 15 that $\mathrm{Re}_x^{1/2}C_{fx}$ increases with β at epilimnion stage which is known as the highest and warmest layer ($S_t = 0$). In addition, a significant decrease in $\mathrm{Re}_x^{1/2}C_{fx}$ is observed with an increase in β at hypolimnion stage which can be referred to as the coolest layer. Mathematically, when $S_t = 0$, this implies that $\Theta(\varsigma) = 1$ and maximum wall temperature at the wall explains the increase in $\mathrm{Re}_x^{1/2}C_{fx}$ since increase in β corresponds to a decrease in yield stress P_y.

5. Conclusion

The boundary layer analysis of non-Newtonian Casson fluid flow over a horizontal melting surface embedded in a thermally stratified medium in the presence of viscous dissipation internal space heat source has been investigated numerically. The effects of the velocity power index, melting parameter, temperature-dependent viscous parameter, Eckert number, thermal conductivity, and magnetic interaction parameter were examined. Conclusions of the present analysis are as follows:

(1) Increase in the magnitude of velocity index parameter leads to a decrease in velocity and increase in temperature due to combine practical influence of the parameter.

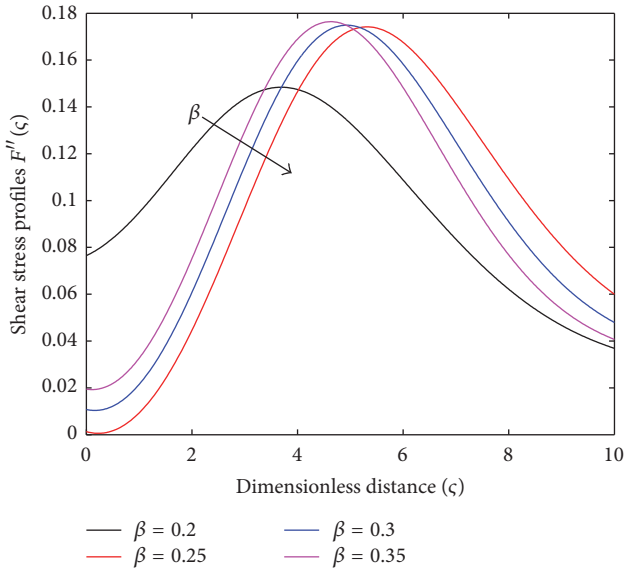

Figure 10: Effect of β on $F(\varsigma)$.

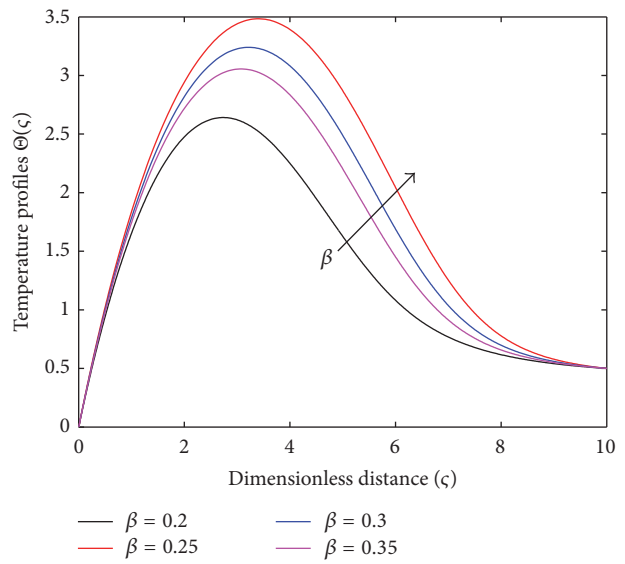

Figure 11: Effect of β on $F'(\varsigma)$.

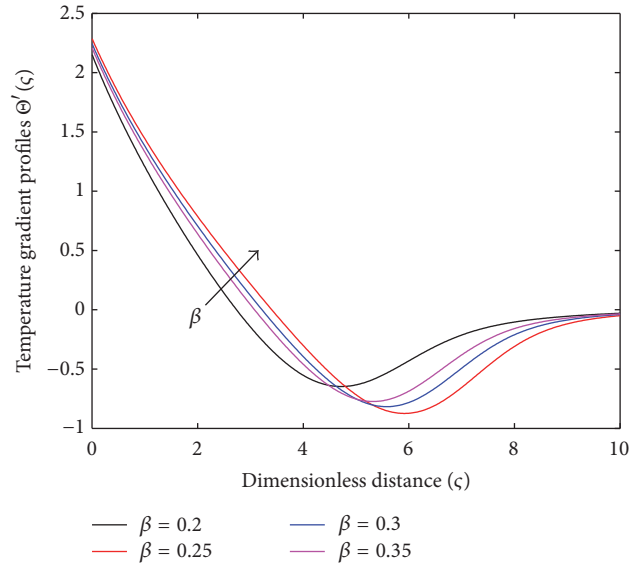

Figure 12: Effect of β on $F''(\varsigma)$.

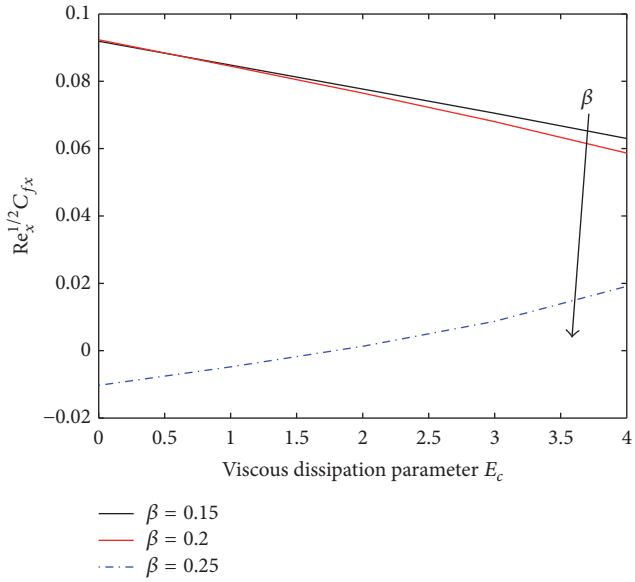

Figure 13: Variations in $\mathrm{Re}_x^{1/2} C_{fx}$ with E_c at various values of β.

(2) $\mathrm{Nu}_x \mathrm{Re}_x^{-1/2}$ decreases with E_c at various values of m within the interval $0.05 \leq m \leq 0.35$. $\mathrm{Re}_x^{1/2} C_{fx}$ decreases with E_c and m.

(3) At various values of viscous dissipation within $0 \leq E_c \leq 4$ and due to the nature of the flow past melting surface, a valid non-Newtonian parameter falls within the interval $0.000001 \leq \beta < 0.21$. Equivalent Newtonian fluid flow is guaranteed for $\beta \geq 0.23$.

(4) Local skin friction coefficient $\mathrm{Re}_x^{1/2} C_{fx}$ increases negligible with S_t when magnitude of β is small. A significant increases in $\mathrm{Re}_x^{1/2} C_{fx}$ is guaranteed with S_t when magnitude of β is large.

(5) In the case of Casson fluid flow over an upper horizontal thermally stratified melting surface of a paraboloid of revolution, decrease in horizontal velocity is guaranteed with an increase m and β.

(6) With an increase in the magnitude of m, the influence of stretching velocity at the wall $U_w = U_o(x + b)^m$ on horizontal and vertical velocities is stronger than that of $y = A(x + b)^{(1-m)/2}$ which describes the immediate fluid's layer next to upper horizontal surface of a paraboloid of revolution due to melting heat transfer.

An extension of the present study to the case of Williamson and Prandtl fluid flow over an upper horizontal thermally stratified melting surface of a paraboloid of revolution

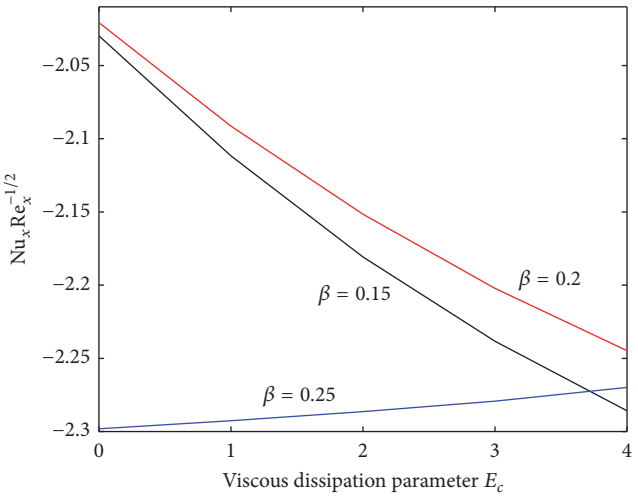

FIGURE 14: Variations in $\mathrm{Nu}_x\mathrm{Re}_x^{-1/2}$ with E_c at various values of β.

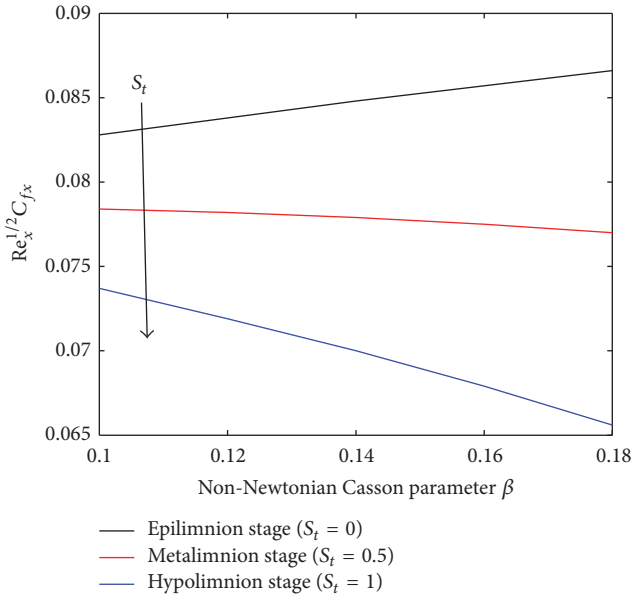

FIGURE 15: Variations in $\mathrm{Re}_x^{1/2}C_{fx}$ with β at various values of S_t.

is hereby recommended. For suitable parametrization to achieve a comparative study, see [7].

Nomenclature

u: Velocity component in x direction
v: Velocity component in y direction
A: Coefficient related to stretching sheet
B_o: Magnetic field strength
C_f: Skin friction coefficient
C_p: Specific heat at constant pressure
x: Distance along the surface
y: Distance normal to the surface
b: Parameter related to stretching sheet
Nu_x: Local Nusselt number
P_r: Prandtl number
q_w: Heat transfer
T: Dimensional fluid temperature
U_w: Stretching velocity at the wall
b_1: Thermal property of the fluid
E_c: Eckert number
f, F: Dimensionless vertical velocity
κ_b: Thermal conductivity of the Casson fluid
m: Velocity power index
T_m: Melting temperature at wall
T_∞: Ambient Temperature
Re_x: Local Reynolds number
β: Non-Newtonian Casson parameter
ξ: Wall thickness parameter
μ_b: Plastic dynamic viscosity
λ^*: Latent heat of the fluid
δ: Melting parameter
θ, Θ: Dimensionless temperature
ϑ: Kinematic viscosity
ξ: Temperature-dependent viscosity parameter
ε: Temperature-dependent thermal conductivity parameter
ρ: Density of Casson fluid
σ: Electrical conductivity of the fluid
$\psi(x, y)$: Stream function.

Competing Interests

The authors declare that they have no competing interests.

References

[1] L. L. Lee, "Boundary layer over a thin needle," *Physics of Fluids*, vol. 10, no. 4, pp. 820–822, 1967.

[2] T. Cebeci and T. Y. Na, "Laminar free-convection heat transfer from a needle," *Physics of Fluids*, vol. 12, no. 2, pp. 463–465, 1969.

[3] S. Ahmad, R. Nazar, and L. Pop, "Mathematical modeling of boundary layer flow over a moving thin needle with variable heat flux," in *Advances in Numerical Methods*, vol. 11 of *Lecture Notes in Electrical Engineering*, pp. 43–54, Springer, Berlin, Germany, 2009.

[4] T. Fang, J. Zhang, and Y. Zhong, "Boundary layer flow over a stretching sheet with variable thickness," *Applied Mathematics and Computation*, vol. 218, no. 13, pp. 7241–7252, 2012.

[5] I. L. Animasaun, "47nm alumina–water nanofluid flow within boundary layer formed on upper horizontal surface of paraboloid of revolution in the presence of quartic autocatalysis chemical reaction," *Alexandria Engineering Journal*, vol. 55, no. 3, pp. 2375–2389, 2016.

[6] I. L. Animasaun and N. Sandeep, "Buoyancy induced model for the flow of 36 nm alumina-water nanofluid along upper horizontal surface of a paraboloid of revolution with variable thermal conductivity and viscosity," *Powder Technology*, vol. 301, pp. 858–867, 2016.

[7] O. Abegunrin, S. Okhuevbie, and I. Animasaun, "Comparison between the flow of two non-Newtonian fluids over an upper horizontal surface of paraboloid of revolution: boundary layer analysis," *Alexandria Engineering Journal*, vol. 55, no. 3, pp. 1915–1929, 2016.

[8] O. D. Makinde and I. L. Animasaun, "Bioconvection in MHD nanofluid flow with nonlinear thermal radiation and quartic autocatalysis chemical reaction past an upper surface of a paraboloid of revolution," *International Journal of Thermal Sciences*, vol. 109, pp. 159–171, 2016.

[9] O. Makinde and I. Animasaun, "Thermophoresis and Brownian motion effects on MHD bioconvection of nanofluid with nonlinear thermal radiation and quartic chemical reaction past an upper horizontal surface of a paraboloid of revolution," *Journal of Molecular Liquids*, vol. 221, pp. 733–743, 2016.

[10] E. Pop, "Energy dissipation and transport in nanoscale devices," *Nano Research*, vol. 3, no. 3, pp. 147–169, 2010.

[11] T. G. Motsumi and O. D. Makinde, "Effects of thermal radiation and viscous dissipation on boundary layer flow of nanofluids over a permeable moving flat plate," *Physica Scripta*, vol. 86, no. 4, Article ID 045003, 2012.

[12] O. D. Makinde, "Analysis of Sakiadis flow of nanofluids with viscous dissipation and Newtonian heating," *Applied Mathematics and Mechanics (English Edition)*, vol. 33, no. 12, pp. 1545–1554, 2012.

[13] M. Abd El-Aziz, "Unsteady mixed convection heat transfer along a vertical stretching surface with variable viscosity and viscous dissipation," *Journal of the Egyptian Mathematical Society*, vol. 22, no. 3, pp. 529–537, 2014.

[14] M. H. M. Yasin, A. Ishak, and I. Pop, "MHD stagnation-point flow and heat transfer with effects of viscous dissipation, Joule heating and partial velocity slip," *Scientific Reports*, vol. 5, Article ID 17848, 2015.

[15] I. L. Animasaun and O. B. Aluko, "Analysis on variable fluid viscosity of non-darcian flow over a moving vertical plate in a porous medium with suction and viscous dissipation," *IOSR Journal of Engineering*, vol. 4, no. 8, pp. 18–32, 2014.

[16] C. S. K. Raju and N. Sandeep, "MHD slip flow of a dissipative Casson fluid over a moving geometry with heat source/sink: a numerical study," *Acta Astronautica*, 2016.

[17] V. J. Rossow, "On the flow of electrically conducting fluid over a flat plate in the presence of a transverse magnetic field," NACA Technical Report 3071, 1957.

[18] H. Alfvén, "Existence of electromagnetic-hydrodynamic waves," *Nature*, vol. 150, no. 3805, pp. 405–406, 1942.

[19] V. M. Soundalgekar and T. V. R. Murty, "Heat transfer in MHD flow with pressure gradient, suction and injection," *Journal of Engineering Mathematics*, vol. 14, no. 2, pp. 155–159, 1980.

[20] R. Rajeswari, B. Jothiram, and V. K. Nelson, "Chemical reaction, heat and mass transfer on nonlinear MHD boundary layer flow through a vertical porous surface in the presence of suction," *Applied Mathematical Sciences*, vol. 3, no. 49–52, pp. 2469–2480, 2009.

[21] S. K. Ghosh, O. A. Bég, and A. Aziz, "A mathematical model for magnetohydrodynamic convection flow in a rotating horizontal channel with inclined magnetic field, magnetic induction and hall current effects," *World Journal of Mechanics*, vol. 1, no. 3, pp. 137–154, 2011.

[22] K. Das, "Radiation and melting effects on MHD boundary layer flow over a moving surface," *Ain Shams Engineering Journal*, vol. 5, no. 4, pp. 1207–1214, 2014.

[23] S. S. Motsa and I. L. Animasaun, "A new numerical investigation of some thermo-physical properties on unsteady mhd non-darcian flow past an impulsively started vertical surface," *Thermal Science*, vol. 19, supplement 1, pp. 249–258, 2015.

[24] O. K. Koriko, T. Oreyeni, A. J. Omowaye, and I. L. Animasaun, "Homotopy analysis of MHD free convective micropolar fluid flow along a vertical surface embedded in non-darcian thermally-stratified medium," *Open Journal of Fluid Dynamics*, vol. 6, no. 3, pp. 198–221, 2016.

[25] B. K. Jha and B. Aina, "Role of induced magnetic field on MHD natural convection flow in vertical microchannel formed by two electrically non-conducting infinite vertical parallel plates," *Alexandria Engineering Journal*, vol. 55, no. 3, pp. 2087–2097, 2016.

[26] B. K. Jha and B. Aina, "MHD mixed convection flow in a vertical pipe with time periodic boundary condition: steady periodic regime," *International Journal of Fluid Mechanics Research*, vol. 43, no. 4, pp. 350–367, 2016.

[27] L. Roberts, "On the melting of a semi-infinite body of ice placed in a hot stream of air," *Journal of Fluid Mechanics*, vol. 4, pp. 505–528, 1958.

[28] C. Tien and Y. Yen, "The effect of melting on forced convection heat transfer," *Journal of Applied Meteorology*, vol. 4, no. 4, pp. 523–527, 1965.

[29] M. Epstein and D. H. Cho, "Melting heat transfer in steady laminar flow over a flat plate," *Journal of Heat Transfer*, vol. 98, no. 3, pp. 531–533, 1976.

[30] R. S. Gorla, A. J. Chamkha, and E. Al-Meshaiei, "Melting heat transfer in a nanofluid boundary layer on a stretching circular cylinder," *Journal of Naval Architecture and Marine Engineering*, vol. 9, no. 1, pp. 1–10, 2012.

[31] K. S. Adegbie, A. J. Omowaye, A. B. Disu, and I. L. Animasaun, "Heat and mass transfer of upper convected maxwell fluid flow with variable thermo-physical properties over a horizontal melting surface," *Applied Mathematics*, vol. 6, no. 8, pp. 1362–1379, 2015.

[32] A. J. Omowaye and I. L. Animasaun, "Upper-convected maxwell fluid flow with variable thermo-physical properties over a melting surface situated in hot environment subject to thermal stratification," *Journal of Applied Fluid Mechanics*, vol. 9, no. 4, pp. 1777–1790, 2016.

[33] I. L. Animasaun, "Melting heat and mass transfer in stagnation point micropolar fluid flow of temperature dependent fluid viscosity and thermal conductivity at constant vortex viscosity," *Journal of the Egyptian Mathematical Society*, 2016.

[34] G. K. Batchelor, *An Introduction to Fluid Dynamics*, Cambridge University Press, Cambridge, UK, 1987.

[35] F. C. Lai and F. A. Kulacki, "The effect of variable viscosity on convective heat transfer along a vertical surface in a saturated porous medium," *International Journal of Heat and Mass Transfer*, vol. 33, no. 5, pp. 1028–1031, 1990.

[36] M. Abd El-Aziz, "Temperature dependent viscosity and thermal conductivity effects on combined heat and mass transfer in MHD three-dimensional flow over a stretching surface with Ohmic heating," *Meccanica*, vol. 42, article 375, 2007.

[37] O. D. Makinde and R. L. Maserumule, "Thermal criticality and entropy analysis for a variable viscosity Couette flow," *Physica Scripta*, vol. 78, no. 1, Article ID 015402, 2008.

[38] M. M. Rahman, M. A. Rahman, M. A. Samad, and M. S. Alam, "Heat transfer in a micropolar fluid along a non-linear stretching sheet with a temperature-dependent viscosity and variable surface temperature," *International Journal of Thermophysics*, vol. 30, no. 5, pp. 1649–1670, 2009.

[39] M. Y. Malik, M. Khan, T. Salahuddin, and I. Khan, "Variable viscosity and MHD flow in Casson fluid with Cattaneo-Christov

heat flux model: using Keller box method," *Engineering Science and Technology, an International Journal*, vol. 19, no. 4, pp. 1985–1992, 2016.

[40] O. D. Makinde, "Heat and mass transfer in a pipe with moving surface: effects of viscosity variation and energy dissipation," *Quaestiones Mathematicae*, vol. 24, no. 1, pp. 93–104, 2001.

[41] I. L. Animasaun, "Casson fluid flow with variable viscosity and thermal conductivity along exponentially stretching sheet embedded in a thermally stratified medium with exponentially heat generation," *Journal of Heat and Mass Transfer Research*, vol. 2, no. 2, pp. 63–78, 2015.

[42] B. K. Jha, B. Aina, and Z. Rilwanu, "Steady fully developed natural convection flow in a vertical annular microchannel having temperature dependent viscosity: an exact solution," *Alexandria Engineering Journal*, vol. 55, no. 2, pp. 951–958, 2016.

[43] M. S. Alam, M. M. Rahman, and M. A. Sattar, "Transient magnetohydrodynamic free convective heat and mass transfer flow with thermophoresis past a radiate inclined permeable plate in the presence of variable chemical reaction and temperature dependent viscosity," *Nonlinear Analysis: Modelling and Control*, vol. 14, no. 1, pp. 3–20, 2009.

[44] T. Hayat, S. A. Shehzad, M. Qasim, and A. Alsaedi, "Mixed convection flow by a porous sheet with variable thermal conductivityand convective boundary condition," *Brazilian Journal of Chemical Engineering*, vol. 31, no. 1, pp. 109–117, 2014.

[45] N. Casson, "A flow equation for pigment oil-suspensions of the printing ink type," in *Rheology of Disperse Systems*, C. C. Mill, Ed., p. 84, Pergamon Press, 1959.

[46] I. L. Animasaun, "Double diffusive unsteady convective micropolar flow past a vertical porous plate moving through binary mixture using modified Boussinesq approximation," *Ain Shams Engineering Journal*, vol. 7, no. 2, pp. 755–765, 2015.

[47] M. M. Rahman and K. M. Salahuddin, "Study of hydromagnetic heat and mass transfer flow over an inclined heated surface with variable viscosity and electric conductivity," *Communications in Nonlinear Science and Numerical Simulation*, vol. 15, no. 8, pp. 2073–2085, 2010.

[48] A. Pantokratoras, "Laminar free-convection over a vertical isothermal plate with uniform blowing or suction in water with variable physical properties," *International Journal of Heat and Mass Transfer*, vol. 45, no. 5, pp. 963–977, 2002.

[49] T. Y. Na, *Computational Methods in Engineering Boundary Value Problems*, Academic Press, New York, NY, USA, 2009.

[50] A. Pantokratoras, "A common error made in investigation of boundary layer flows," *Applied Mathematical Modelling*, vol. 33, no. 1, pp. 413–422, 2009.

[51] J. Kierzenka and L. F. Shampine, "A BVP solver based on residual control and the Maltab PSE," *ACM Transactions on Mathematical Software*, vol. 27, no. 3, pp. 299–316, 2001.

[52] F. S. Gökhan, *Effect of the Guess Function & Continuation Method on the Run Time of MATLAB BVP Solvers*, Edited by C. M. Ionescu, 2011.

[53] M. Mustafa, T. Hayat, I. Pop, and A. Aziz, "Unsteady boundary layer flow of a Casson fluid due to an impulsively started moving flat plate," *Heat Transfer—Asian Research*, vol. 40, no. 6, pp. 563–576, 2011.

[54] I. L. Animasaun, "Effects of thermophoresis, variable viscosity and thermal conductivity on free convective heat and mass transfer of non-darcian MHD dissipative Casson fluid flow with suction and nth order of chemical reaction," *Journal of the Nigerian Mathematical Society*, vol. 34, no. 1, pp. 11–31, 2015.

[55] A. Jasmine Benazir, R. Sivaraj, and M. M. Rashidi, "Comparison between casson fluid flow in the presence of heat and mass transfer from a vertical cone and flat plate," *Journal of Heat Transfer*, vol. 138, no. 11, Article ID 112005, 2016.